

put forward by Frank and Wen, water molecules become ordered around the organic molecule with an increase in hydrogen bonding in this region. Any solute which increases the stability of the water clusters (as measured, for example, by an increase in the molecular reorientation time of liquid water) is said to be structure making. Speaking broadly, nonpolar molecules and large ion salts are structure makers. Small ion salts, as, for example, the alkali metal halides, are generally structure breakers.

A good indication of the effect of solutes on solvent structure is given by their effect on the dielectric dispersion wavelength.^{16b,17} Interestingly the relative effects of the tetraalkylammonium and alkali metal halides on the structure of water, as measured by changes in the relaxation wavelength, are almost precisely the same as their relative effects on the rate of detritiation of the malononitriles. The effects of low mole fractions of alcohol and dioxane are similarly correlated. In other words, additives which increase water structure (the organic solvents and the tetraalkylammonium salts) lead to an increased rate of detritiation; the reverse is true for structure breakers. The relative effects of chloride and bromide ions as observed for the tetramethylammonium and tetraethylammonium halides are also in agreement with their expected effects on solvent structure (bromide ion is thought to be a more effective structure breaker).

The particular way in which enhanced water structure increases the rate of proton removal from a malononitrile can be persuasively explained as follows. In aqueous solution the malononitriles are probably surrounded by clusters of hydrogen-bonded solvent molecules. Proton transfer occurs to a water molecule in one of these neighboring clusters, and a solvated hydronium ion is formed. It is well known that the hydronium ion is heavily solvated in aqueous solution as

(17) G. H. Haggis, J. B. Hasted, and T. J. Buchanan, *J. Chem. Phys.*, **20**, 1952 (1952).

a large hydrogen-bonded complex.¹⁸ It is also likely that the almost fully formed hydronium ion of the transition state is stabilized by several solvent molecules. If proton transfer from malononitrile occurs to a cluster of water molecules, stabilization of the forming hydronium ion by solvent rearrangement within this cluster probably occurs. One would then expect salting-in of the transition state and increased rates in a solvent with greater structure since the stabilization of the hydronium ion is then accomplished more readily. This is observed in solutions of tetraalkylammonium salts and in solutions containing low mole fractions of organic solvents. In the presence of considerably larger mole fractions of organic solvents, however, the water structure is disrupted and this probably contributes to the decrease in rate which is then observed.

In water solutions, the detritiations of malononitrile and *tert*-butylmalononitrile occur with entropies of activation of -22 and -21 eu, respectively, when k values are in $M^{-1} \text{ sec}^{-1}$ units. These values are about a dozen entropy units more negative than normal, *i.e.*, than the value for a simple "collision theory" frequency factor. The most obvious explanation is that the dipolar transition states are more potent structure makers than the reactants themselves, *i.e.*, that this large negative entropy term is primarily a measure of the enhanced water structure which develops on formation of the transition state. From this point of view, addition of a structure maker such as tetraethylammonium bromide should decrease the required further structure making and hence cause a rate acceleration. The implication of this analysis, that the principal effect of additives will be on the entropies of activation, is now under investigation.

Acknowledgment. We wish to thank Mrs. Sue Garcia and Mrs. Diane Parchomchuk for technical assistance.

(18) B. E. Conway, "Modern Aspects of Electrochemistry," J. O'M. Bockris and B. E. Conway, Ed., Butterworths, Washington, D. C., 1964, p 43; M. Eigen, *Angew. Chem., Int. Ed. Engl.*, **3**, 1 (1964).

Stopped-Flow Nuclear Magnetic Resonance Spectroscopy

John Grimaldi, John Baldo, Cecil McMurray, and Brian D. Sykes*

Contribution from the Department of Chemistry, Harvard University, Cambridge, Massachusetts 02138. Received May 30, 1972

Abstract: A rapid mixing cell for nmr and a stopped-flow nmr spectrometer have been constructed. Stopped-flow nmr has been applied to the study of the reaction $\text{Ni}(\text{NH}_3)(\text{H}_2\text{O})_5^{2+} + \text{H}_3\text{O}^+ \rightarrow \text{Ni}(\text{H}_2\text{O})_6^{2+} + \text{NH}_4^+$. The rate constant obtained is in excellent agreement with the rate constant obtained using optical stopped-flow techniques. Several conditions for the applicability of stopped-flow nmr are discussed.

Nmr methods have been widely applied to the study of reactions in chemical and biochemical systems.^{1,2} Virtually all of the applications, however, have been studies of exchange reactions at equilibrium.

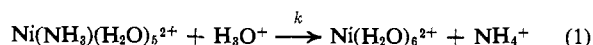
(1) C. S. Johnson, *Advan. Magn. Resonance*, **1**, 33 (1965).
(2) B. D. Sykes and M. Scott, *Annu. Rev. Biophys. Bioeng.*, **1**, 251 (1972).

The advent of Fourier transform nmr techniques, which have greatly reduced the time required to obtain an nmr spectrum,³ has focused attention on the possibility of using nmr to study rapid irreversible chemical reactions (and transient phenomena such as CIDNP).

(3) R. R. Ernst and W. A. Anderson, *Rev. Sci. Instrum.*, **37**, 93 (1966).

In general, the number of species identified in any chemical reaction is limited by two factors: (1) the time interval over which the reaction is followed, and (2) the method of detection. Stopped-flow methods have the advantage that they greatly shorten the time range during which the dynamics of a reaction can be studied. Using optical detection systems stopped-flow methods have been extensively applied to the study of rapid chemical and biochemical reactions.⁴ Nmr can be used as a detection method for this large class of reactions if the reaction can be initiated within the nmr spectrometer and spectra obtained within a time less than the half-time of the reaction. As with all other applications, the great advantage of nmr over other detection methods is that all of the species involved in a reaction can often be identified and followed independently.

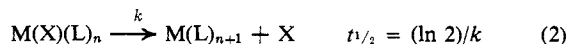
In this paper the development of a rapid mixing cell and stopped flow nmr spectrometer is described. In addition, stopped flow nmr is applied to the study of the reaction



This reaction was chosen for the following reasons: (1) the rate constant can be determined independently using optical stopped flow techniques⁵ and compared with the rate constant determined using nmr, (2) the half-time of the reaction is in an appropriate time range, and (3) the strong H₂O resonance (which is a weighted average of many sites) provides a probe for the reaction, broadening as the reaction progresses. Since only one resonance was observed during the reaction and the main purpose of this paper was to demonstrate the feasibility of using nmr to study reactions on the millisecond time scale, continuous wave (CW) methods were used rather than Fourier transform (FT) methods in this study. CW methods are more easily applied when only one resonance frequency is to be monitored; this allows the continuous observation of the resonance during the reaction. On the other hand, FT methods are advantageous when several resonances spanning a wide spectral range are to be observed. A preliminary report of kinetic studies of the reaction of the enzyme lysozyme with its natural tetrasaccharide substrate from cell walls using FT techniques has appeared,⁶ and these results along with similar studies of other enzyme reactions will be presented in detail elsewhere.⁷⁻⁹ The time scale of these FT studies, however, and that of the stopped-flow nmr studies described by Sudmeier and Pesek,¹⁰ are much longer than the time scale of the studies described herein.

Theory

In this section a line-shape expression is derived for nuclei on a ligand L involved in a first-order reaction of the type



(4) Q. H. Gibson, *Methods Enzymol.*, **16**, 187 (1969), and references therein.

(5) G. A. Melson and R. G. Wilkins, *J. Chem. Soc.*, 4208 (1962).

(6) B. D. Sykes, S. L. Patt, and D. Dolphin, *Cold Spring Harbor Symp. Quant. Biol.*, **36**, 29 (1971).

(7) S. L. Patt, D. Dolphin, and B. D. Sykes, submitted for publication.

(8) J. J. Mieyal, R. H. Abeles, S. L. Patt, and B. D. Sykes, submitted for publication.

(9) J. J. Grimaldi and B. D. Sykes, submitted for publication.

(10) J. L. Sudmeier and J. J. Pesek, *Inorg. Chem.*, **10**, 860 (1971).

where the line widths and/or chemical shifts of the nuclei are different for the ligand L in different environments (free in solution, bound to M, and bound to MX) and under conditions such that (1) the rate of exchange of the ligand L between free solution and either complex M(X)(L)_n or M(L)_{n+1} is rapid

$$1/\tau_i > 1/T_{2i}, \Delta\omega_i$$

where τ_i , T_{2i} , and $\Delta\omega_i$ are exchange lifetime, transverse relaxation time, and chemical shift, respectively, for nuclei on the ligand L in site i , and (2) the rate of the reaction is slow

$$1/T_1(t) > 1/t_{1/2}$$

where $1/T_1(t) = \sum_i P_i(t)/T_{1i}$, T_{1i} is the longitudinal relaxation time for site i , and $P_i(t)$ is the fractional population of site i at time t . These conditions are satisfied for the reaction studied in this paper. Other possible situations are considered in the Discussion section.

Under the above conditions the signal intensity $I(t)$ for a nucleus on the ligand L can be written in the absorption mode as¹¹

$$I(t) = C \frac{\Delta\nu(t)}{[\Delta\nu(t)]^2 + 4[\nu - \nu_0(t)]^2} \quad (3)$$

where $\Delta\nu(t) = \sum_i P_i(t)\Delta\nu_i$, ν is the observing frequency (in Hz), $\nu_0(t) = \sum_i P_i(t)\nu_{0i}$, ν_{0i} is the resonance frequency in site i , and C is a constant.

For a first-order reaction

$$\Delta\nu(t) = \Delta\nu(0)e^{-kt} + \Delta\nu(\infty)(1 - e^{-kt}) = \Delta\nu(\infty) + [\Delta\nu(0) - \Delta\nu(\infty)]e^{-kt} = \Delta\nu(\infty) + ze^{-kt} \quad (4)$$

where $\Delta\nu(0) = \sum_i P_i(0)\Delta\nu_i$ and $\Delta\nu(\infty) = \sum_i P_i(\infty)\Delta\nu_i$, and

$$\nu_0(t) = \nu_0(0)e^{-kt} + \nu_0(\infty)(1 - e^{-kt}) = \nu_0(\infty) + [\nu_0(0) - \nu_0(\infty)]e^{-kt} = \nu_0(\infty) + \delta e^{-kt} \quad (5)$$

where $\nu_0(0) = \sum_i P_i(0)\nu_{0i}$ and $\nu_0(\infty) = \sum_i P_i(\infty)\nu_{0i}$.

Substituting eq 4 and 5 into eq 3

$$I(t) = C \frac{\Delta\nu(\infty) + ze^{-kt}}{[\Delta\nu(\infty) + ze^{-kt}]^2 + 4[\nu - \nu_0(\infty) - \delta e^{-kt}]^2} \quad (6)$$

By setting $\nu = \nu_0(\infty)$ eq 6 becomes

$$I(t) = C \frac{\Delta\nu(\infty) + ze^{-kt}}{[\Delta\nu(\infty) + ze^{-kt}]^2 + 4\delta^2 e^{-2kt}} \quad (7)$$

At $t = \infty$

$$C = I(\infty)\Delta\nu(\infty) \quad (8)$$

giving

$$I(t) = I(\infty)\Delta\nu(\infty) \left\{ \frac{\Delta\nu(\infty) + ze^{-kt}}{[\Delta\nu(\infty) + ze^{-kt}]^2 + 4\delta^2 e^{-2kt}} \right\} \quad (9)$$

where $I(\infty)$ and $\Delta\nu(\infty)$ are experimentally measurable quantities. If δ is known or if $4\delta^2 \ll [\Delta\nu(0)]^2$, then the experimental data can be fitted to eq 9 treating z and k as parameters.

Experimental Section

The stopped flow nmr (Figure 1) consists of three units: the rapid mixing system, the spectrometer, and the transient recorder.

(11) T. J. Swift and R. E. Connick, *J. Chem. Phys.*, **37**, 307 (1962).

56.4 MHz Stopped Flow NMR Spectrometer

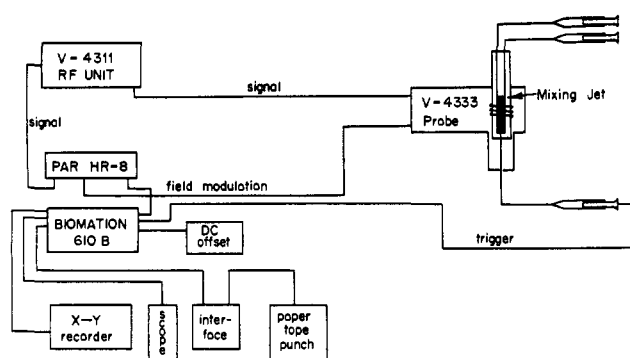


Figure 1. Block diagram of the stopped flow nmr spectrometer.

The rapid mixing system consists of a driving syringe block, a rapid mixing cell, and a stopping syringe. The syringe blocks are of standard design. Both driving syringes and the stopping syringe were 2-cc B&D syringes. The driving syringes were pushed by hand. Flow was arrested when the stopping syringe hit a solid support, the position of which could be adjusted to allow a given volume to be pushed for each transient. The transient recorder was triggered by the contact of the stopping syringe with the solid stopping block. The rapid mixing cell (Figure 2) was made from a Rexalite rod 5 mm in diameter. Mixing jets were drilled tangentially to the observation tube to create a turbulent motion of the reactant solutions. This provides good mixing as well as efficient removal of the previously reacted solution from the observation region of the cell. Tangential jets proved to be superior to a simple T mixer. The top of the mixing cell was fitted with small diameter glass tubing, and these were connected *via* rigid plastic tubing to the driving syringes. A 5-mm nmr tube was also fitted to the top of the cell to provide support for the input tubes. A small glass tube was epoxyed to the bottom of the cell and this was connected to the stopping syringe *via* Teflon tubing. The position of the cell with respect to the receiver coil was adjusted to give the optimum signal and the smallest dead time. The volume of the observation cell was approximately 100 μ l, and the total solution volume pushed through the cell for each transient was approximately 200 μ l. The cell does not spin.

The spectrometer consists simply of a Varian HR 56.4-MHz nmr spectrometer where the output of the V-4311 rf unit is fed into a PAR HR-8 lock-in amplifier. The maximum filtering used was the -12 db/octave 3-msec filtering of the PAR. Signals were recorded digitally with a Biomation 610B transient recorder. The stored and digitized transient could be displayed on the oscilloscope, plotted on the X-Y recorder, or punched on paper tape.

To obtain a transient, the magnetic field is swept to the center of the H_2O resonance (center band) and the phases of the V-4311 and PAR are adjusted to give the optimum absorption signal. It was no problem in our case to sit on resonance since the H_2O resonance was broad (34-42 Hz). Power levels are set well below saturation. After these adjustments are made the driving syringes are pushed and the transient recorder is triggered. A typical transient is shown in Figure 3.

Figure 4 illustrates the above and provides a test of whether or not a shift in resonance frequency occurs during our reaction. Two identical mixing experiments are shown in this figure. During the first mixing experiment a transient was recorded on a storage oscilloscope. Curve A shows the initial portion of this transient and the horizontal line B shows the trace at $t = \infty$. For the second mixing experiment the driving syringe was set to trigger a triangular magnetic field ramp (applied to the sweep coils of the probe) which swept the magnetic field first off resonance, then through resonance, and finally back onto resonance during the reaction. The resulting signal for the initial portion of the reaction is curve C. Curves A and C coincide when the magnetic field ramp is on resonance. Curve D shows the same signal at $t = \infty$, and curve E shows the ramp. Any change in the absorption peak position between curves C and D can be used to determine the chemical shift of the resonance during the reaction.

Optical stopped-flow measurements were made using identical solutions as in the nmr method. These measurements were made on a Durrum-Gibson stopped-flow spectrophotometer at 610 nm over a temperature range of 20-25°. A typical transient is shown in

to driving syringes

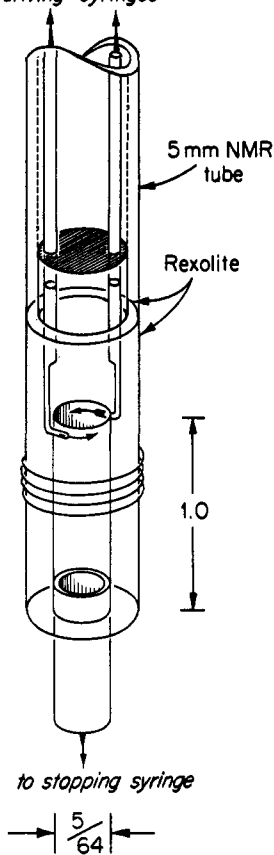


Figure 2. The rapid mixing cell (not drawn to scale). The two inputs (which are connected to the driving syringes *via* rigid plastic tubing) are 0.059-in. (o.d.) glass tubing and are epoxyed into two holes at the top of the Rexalite cell. These holes constrict to 0.020 in. in diameter and terminate in 0.020-in. mixing jets which are tangential to the $5/64$ -in. diameter observation chamber. The arrows indicate the tangential flow of the reactants during mixing. Previously reacted solution is exited through a $5/64$ -in. (o.d.) glass tube epoxyed to the bottom of the cell. This tube is connected to the stopping syringe *via* Teflon tubing.

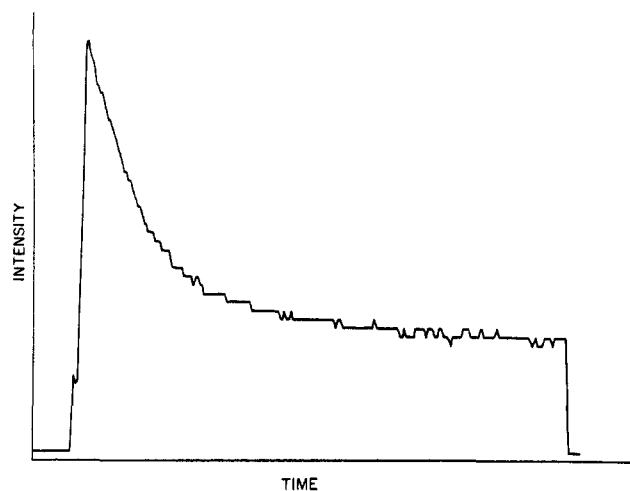


Figure 3. A typical transient as plotted on the X-Y recorder by the Biomation 610B. The horizontal lines at the beginning and the end of the plot are not part of the transient. The correct offset is indicated in Figure 6. The time elapsed during this transient is 1.12 sec. The coarseness of the plot reflects the 6-bit digitization.

Figure 5. The observed optical density reflects the change in concentration of the chromophore $Ni(H_2O)_6^{2+}$.

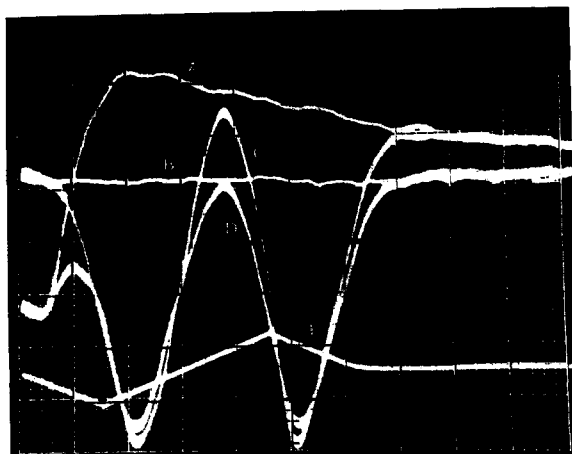


Figure 4. Oscilloscope trace of two identical mixing experiments. The first experiment (curves A and B) shows the initial portion of the transient (curve A) and the trace at $t = \infty$ (curve B). During the second experiment (curves C and D) a ramp (curve E) triggered by the stopping syringe was applied to the sweep coils of the probe. This ramp swept the magnetic field initially off resonance, then through resonance, and finally back onto resonance. The resulting signal for the initial portion of the reaction is shown by trace C and that at time $t = \infty$ by trace D. After the ramp is terminated, curves A and C and curves B and D coincide. One-half cycle of the ramp corresponds to a sweep width of 64 Hz. Scales: $x = 20$ msec/div; $y = 0.2$ V/div.

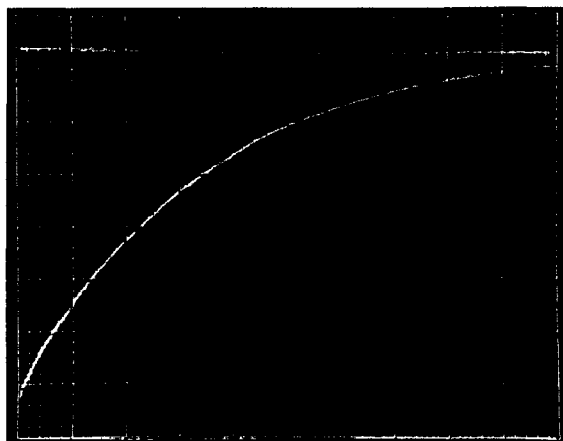


Figure 5. Oscilloscope trace of an optical stopped flow experiment (25°). Both traces show per cent transmission at 610 nm. The lower trace is the kinetic transient, and the upper trace is the infinity reading. Scales: $x = 50$ msec/div, $y = 20$ mV/div. Baseline (zero graticule) offset is 0.25 V; filter, 5 msec.

The nickel amine solution¹² was prepared by adding 6.3 ml of 30% ammonium hydroxide to 158 ml of 1.14 M nickel nitrate. After the addition of 80 g of ammonium nitrate, the solution was brought to 500 ml. The total concentration of Ni^{2+} in this solution was 0.36 M. This solution was put in one driving syringe. In the second driving syringe 0.4 M nitric acid was placed.

Results

The mixing of ~ 0.36 M $\text{Ni}(\text{NH}_3)(\text{H}_2\text{O})_5^{2+}$ with 0.40 M HNO_3 gave a transient which was digitized. The parameters z and k of eq 9 were determined by obtaining a best fit to the data with the assumption that $\delta = 0$. A nonlinear least-squares program¹³ was used to do the fitting. The term containing δ in the denominator

(12) C. S. Garner and J. Bierrum, *Acta Chem. Scand.*, **15**, 2055 (1961).

(13) N. Arley and K. Randerbuck, "Introduction to Theory of Probability & Statistics," Wiley, New York, N. Y., 1950, Chapter 12.

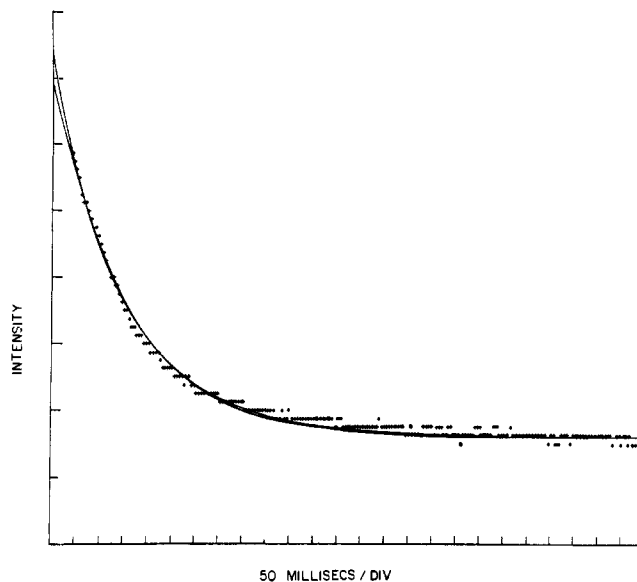


Figure 6. Nonlinear least-squares fit to a stopped flow nmr transient. The +s are the digitized experimental points. The curve with the higher intercept is the fit to eq 9 with $\delta = 0.0$ Hz, and the curve with the lower intercept has $\delta = 4.0$ Hz. The rate constants are 5.9 and 6.4 sec^{-1} , respectively. Each division on the intensity scale is 0.25 V. The intensity at $t = \infty$ is 5.1 V.

in eq 9 can be neglected if $4\delta^2 \ll [\Delta\nu(\infty) + z]^2$. From Figure 4 an upper limit for the shift in resonance frequency at the beginning of the transient is 4 Hz. For reaction 1 at the concentrations specified the measured value of the final line width is $\Delta\nu(\infty) \cong 42$ Hz, and the value for the change in line width during the reaction determined by the computer fit assuming $\delta = 0$ is $z \cong -8$ Hz. The above condition therefore becomes $4\delta^2 \lesssim 64 \ll 1156$. Furthermore, the nonlinear least-squares fit of the digitized transient to eq 9 with $\delta \neq 0$ gives a poorer fit than with $\delta = 0$. Figure 6 is a computer plot of transient 2 (Table I) with the fits corresponding to $\delta = 0$ and $\delta = 4$ Hz. The rate constants k obtained were $k = 5.9$ and $k = 6.4$ sec^{-1} for $\delta = 0$ and $\delta = 4$ Hz, respectively. The average of the nine runs listed in Table I is 6.2 ± 0.1 sec^{-1} . All runs were

Table I. Nmr

Run	k , sec^{-1}
1	6.7
2	5.9
3	6.4
4	5.9
5	6.0
6	6.4
7	6.7
8	6.6
9	5.5
Av	6.2 ± 0.1

at ambient probe temperature ($23 \pm 1^\circ$). No transient was observed for the mixing of 0.3 M $\text{Ni}(\text{H}_2\text{O})_6^{2+}$ with H_2O where the change in line width upon dilution occurs in a time short compared to the response time of the spectrometer ($\gtrsim 3$ msec).

The optical stopped flow results over the temperature range 20 – 25° are listed in Table II. The rate constants

Table II. Optical Results

$T, ^\circ\text{C}$	k, sec^{-1}
25.9	7.1 ± 0.5
22.7	5.4 ± 0.5
20.1	4.5 ± 0.5

range from $4.5 \pm 0.5 \text{ sec}^{-1}$ (20.1°) to $7.1 \pm 0.5 \text{ sec}^{-1}$ (25.0°).

Discussion

Agreement between the optical and nmr results is excellent. The nmr value for the rate constant ($k = 6.2 \pm 0.1 \text{ sec}^{-1}$, $23 \pm 1^\circ$) agrees with the optical value ($k = 5.4 \pm 0.5 \text{ sec}^{-1}$, 22.7°), and both results are in agreement with the literature value.⁵ This conclusion indicates that nmr can indeed be used to study rapid irreversible chemical reactions with half-times in the range of 10 msec (approximately the "dead" time of the instrument) or greater under the conditions stated in the theory section: (1) $1/\tau_1 \gg T_{2i}, \Delta\omega_i$; (2) $1/T_1(t) \gg 1/t_{1/2}$.

Condition 1 is not in general necessary. If it is satisfied, as in the present case, then only one resonance is observed for any given nucleus corresponding to the weighted average of the sites possible for the nucleus during the reaction. This situation has the advantage that a strong resonance can be used to probe concentration changes of a site of low concentration if the relaxation time, for example, in that site is very much shorter than the relaxation times corresponding to the other sites. If condition 1 is not satisfied, then separate resonances will be observed for each site. This clearly provides additional information about the environment of the nucleus in each site such as the chemical shifts, allows each site to be followed independently during the reaction, and permits the observation of changes in more detailed parameters such as coupling constants during the reaction.^{6,7} Fourier transform techniques are of great advantage in following reactions under conditions where several resonances are observed.

Condition 2 is sufficient to ensure that the magnetization is able to follow concentration changes in the system and that the reaction itself is not a relaxation mechanism for the nuclear spin system. Under these conditions each resonance can either be followed continuously using CW methods or the complete spectrum can be sampled at various times using Fourier transform

methods. The Fourier transform method involves the application of a series of rf pulses to the sample during the reaction, and the digitization and storage onto magnetic tape of the free induction decay following each pulse. The resulting free induction decays, when retrieved and Fourier transformed at the end of the reaction, provide the complete spectrum at various times during the reaction.⁷ While Fourier transform techniques have the advantage of being able to follow all of the resonances simultaneously, only a finite number of free induction decays can be digitized and stored during a reaction, so that the range of measurable rate constants is further limited by the criteria

$$n(\text{AT} + \text{TT} + \text{PD}) \lesssim t_{1/2} \quad (10)$$

where n is the number of spectra desired, AT is the acquisition time for the free induction decay ($\sim 1/T_2$), TT is the time required to transfer the free induction decay onto magnetic tape, and PD is the delay time between pulses ($\text{AT} + \text{PD} \gtrsim 3T_1$) to allow the magnetization to return to equilibrium. On the other hand, for CW methods where only one resonance frequency is monitored, condition 2 can be relaxed to

$$1/T_2(t) > 1/t_{1/2}$$

under the conditions that (1) the magnetization is not saturated ($M_z = M_0$) and (2) the reactants are polarized in the magnetic field before mixing. The time required for polarization in the magnetic field seems to account for the "dead" time of the present instrument ($T_1 = 10 \times 10^{-8} \text{ sec}$). If condition 2 is not satisfied the reaction itself becomes a relaxation mechanism for the nuclear spin system and the analysis becomes more difficult. This area is presently under investigation.

Acknowledgments. The authors thank Professor W. Lipscomb for support, Professor F. Westheimer for the use of his optical stopped-flow apparatus, William Hull for providing the nonlinear least-squares program, Joel Cook for computing assistance, Emil Sefnar for assistance in machining the cell, Hampar Janjigian for invaluable assistance with the nmr spectrometer, the National Institutes of Health for financial support (Grant GM-17190 (B. D. S.), GM-06920 (W. L.), and NIH Training Grant Fellowships (J. G. and J. B.)), the Alfred P. Sloan Foundation for financial support (to B. D. S. in the form of an A. P. Sloan Fellowship, 1971-1973), and the Wellcome Foundation for a travel grant (C. M.).